

Influence of manufacturing induced defects on damage initiation and propagation in carbon/epoxy NCF laminates

P. A. Carraro, L. Maragoni & M. Quaresimin

To cite this article: P. A. Carraro, L. Maragoni & M. Quaresimin (2015) Influence of manufacturing induced defects on damage initiation and propagation in carbon/epoxy NCF laminates, *Advanced Manufacturing: Polymer & Composites Science*, 1:1, 44-53, DOI: [10.1179/2055035914Y.0000000004](https://doi.org/10.1179/2055035914Y.0000000004)

To link to this article: <https://doi.org/10.1179/2055035914Y.0000000004>



© 2015 The Author(s). Published by Taylor & Francis



Published online: 02 Jan 2015.



Submit your article to this journal [↗](#)



Article views: 1604



View related articles [↗](#)



View Crossmark data [↗](#)



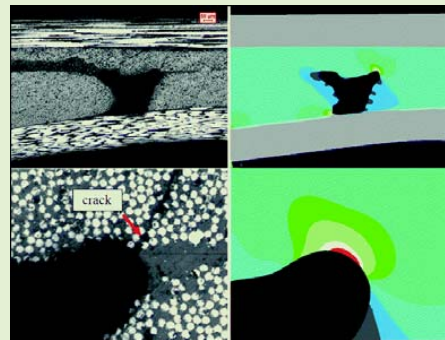
Citing articles: 4 View citing articles [↗](#)

Influence of manufacturing induced defects on damage initiation and propagation in carbon/epoxy NCF laminates

P. A. Carraro, L. Maragoni and M. Quaresimin*

Università degli Studi di Padova – Dipartimento di Tecnica e Gestione dei Sistemi Industriali, Stradella San Nicola 3, 36100 Vicenza, Italy

Abstract In the present work, two sets of NCF carbon/epoxy laminates have been produced via liquid infusion molding, with the aim to investigate the influence of some process parameters on damage initiation and propagation in composite laminates. In the first set the resin was degassed before infusion and the bleeding time was large. In the second set the resin was not degassed and the bleeding time was kept very short. Microscopy analyses revealed an evident void content in the second set of panels, whereas no voids were detectable in the first one. Incremental static tests on cross-ply specimens and DCB tests on $[(90/0)_3]_S$ and $[(+45/-45)_3]_S$ laminates obtained with the two processes were carried out, with the aim to characterise the influence of voids on damage initiation and propagation. Tensile tests revealed that the multiple cracking process in cross-ply laminates was detrimentally affected by the presence of defects. Conversely, DCB tests showed a negligible influence of the presence of defects on the mode I fracture toughness, its propagation value being even higher in the specimens with voids. Damage mechanisms were carefully analyzed to deeply understand the role of voids mainly in the crack initiation process. Finite element analyses carried out considering the actual geometry of voids showed that their local shape, and the related stress/strain concentration, are fundamental parameters to properly describe this phenomenon.



Keywords Vacuum infusion, Voids, Interlaminar fracture toughness, Crack density, Delamination

Cite this article P. A. Carraro, L. Maragoni and M. Quaresimin. *Adv. Manuf.: Polym. Compos. Sci.*, 2015, 1, 44-53

Introduction

Owing to the intrinsic nature of composites, it is extremely difficult and expensive to obtain defects-free components with such materials; in particular, the presence of microscopic voids is nearly unavoidable in complex structures. In processes where liquid resin is used, like RTM and infusion, voids form when air is entrapped as a result of the different resin flow inside the fibre bundles and in the channels between the bundles. Void content depends on the process parameters and conditions, such as resin degassing, temperatures, pressures, and infusion time (see Refs. 1–4 among the others).

The presence of microscopic voids in a composite component can be detrimental for its mechanical intra-laminar and inter-laminar properties.

The influence of voids on the inter-laminar fracture toughness was investigated by Asp and Brandt.⁵ They reported that a small amount of voids (~1% in volume) had

a slightly deleterious or no effect respectively for Mode I and Mixed Mode loading, on the critical Energy Release Rate (ERR, or G) at crack growth initiation for a $0^\circ/5^\circ$ interface. In both cases, an increase of the critical ERR G_c was instead found for crack propagation in the presence of voids due to the occurrence of ply bridging phenomena under Mode I and multiple crack planes at the main crack tip under Mixed Mode loading. In Mode II, instead, voids appeared not to influence the critical ERR. Olivier *et al.*⁶ found instead that for a larger amount of voids (5% in volume), the G_c at crack propagation sensibly decreased for a $0^\circ/0^\circ$ interface under Mode I loading.

The effect of voids on the inter-laminar shear strength (ILSS) has been analysed by several researchers in the literature.^{6–16} Some works^{7,10,14,15} report a linear relation between the ILSS and void volume fraction. However, clear conclusions regarding the influence of voids on this inter-laminar property are hard to draw, it being largely dependent on the materials used, and the laminate stacking sequence.

*Corresponding author, email marino.quaresimin@unipd.it

The effect of voids on the in-plane properties of composites has been studied in terms of tensile, compressive and flexural behaviour.

Concerning the tensile behaviour, the experimental results from Olivier *et al.*⁹ highlighted that the fiber-dominated properties were those less affected by the presence of voids, whereas the behaviour in the transverse direction resulted to be more influenced. Varna *et al.*¹⁷ showed that for larger void content the initiation of the first transverse crack in UD specimens containing a small amount of weft fibres occurred at lower loads and the strain to failure resulted to be larger. However, the influence of voids on tensile modulus and strength was found to depend also on the plies architecture.¹⁸ Huang and co-authors¹⁹ tested autoclave moulded cross-ply laminates obtained with different process parameters resulting in different void contents. They observed a clear dependence of the crack density evolution under static loading on the process parameters, even if this behaviour was not related to the amount or size of voids in the transverse plies.

The compressive strength of composites is also strongly influenced by voids, as shown in Refs. 8, 19 and 20. However, the extent of the void influence varied with the material adopted and the laminate lay-up.

The studies carried out on the flexural behaviour in the presence of voids^{9,15,22-24} did not lead to clear conclusions, with a large variability of the sensitivity of the material performance on the void content. Relating the composite material performance to the global void volume content, as done in the majority of the works, may be too simplistic in the presence of bending loads, since in such cases also the voids spatial distribution plays a fundamental role.

Studies on the influence of voids on the fatigue behaviour of composites can be found in Refs. 14, 22, 25-28. S-N curves were found to be shifted towards shorter fatigue life and steeper in the presence of voids both for tension-tension and compression-compression loading conditions.²⁵⁻²⁷ The same trend was found in presence of bending loads for unidirectional^{22,28} and woven laminates.¹⁴ A linear trend was reported between the fatigue life of [0/45/-45]_{3S} laminates and the size of the largest defect in critical positions by Lambert *et al.*,²⁹ whereas no clear trend appeared to exist between fatigue life and global void content or the largest defect in the whole specimen. Lambert and co-authors²⁹ presented an interesting, though qualitative, analysis of fatigue damage evolution, allowing the authors to identify which were the critical plies in which the presence of voids played a deleterious role. In their study of the inter-laminar tensile strength (ILTS) under fatigue, Seon *et al.*³⁰ correlated instead the life reduction under cyclic loading to the presence of a single void in critical position. Recently, Sisodia and co-authors³¹ analysed the fatigue damage evolution in multidirectional laminates, showing that the density of off-axis cracks, and the subsequent stiffness degradation, were higher in the presence of voids.

Several works have been done with the aim to model the influence of voids on the mechanical properties of composite materials. Models based on finite elements method, by

far the most used, were proposed to calculate the stress concentration factor in the presence of a void and the resulting tensile strength,²⁵ to calculate the ILSS in the presence of a single void,¹¹ to analyze the shear strength³² and to study the decrease in elastic properties as a function of void content,^{33,34} obtaining good agreement with experimental results through the analysis of a unit cell.³³ Some analytical models too were developed in literature, in particular to justify the larger strain to failure in the presence of voids under transverse loading (from a *shear lag* analysis),¹⁷ to predict the ILSS¹³ and flexural resistance (through a modification of Mar-Lin criterion)²³ and to study the effect of voids at the interface between plies on the fracture toughness.³⁵ A statistical model was also developed by Huang *et al.*¹⁹ to predict crack density evolution in cross-ply laminates. This model can be adopted to obtain the statistical distribution of the transverse strength for different process parameters, even if the authors did not correlate the so obtained distributions to the amount of voids present in the laminates.

From the analysis of the scientific literature and despite the amount of experimental data, it can be seen that it is still hard to draw quantitative correlations of general validity between the presence of voids and the mechanical properties of composite materials. Concerning the static and fatigue behavior, the influence of voids has been found to be strongly dependent on the materials adopted and the laminate stacking sequence. Damage evolution in multidirectional laminates is indeed a quite complex phenomenon, characterised by the initiation and propagation of off-axis cracks which then lead to the onset of delamination and final failure. Therefore, both intra-laminar and inter-laminar properties play a fundamental role in the development of damage under static and fatigue loading. As mentioned before, these properties are strongly influenced by the presence of voids. In this scenario, understanding the effect of voids on damage mechanisms leading to the formation and propagation of intra-laminar and inter-laminar cracks is essential. In addition, considering their geometry, size and distribution instead of just their global content could probably bring to an improvement in this direction. In the authors' view, this mechanisms based approach is fundamental to provide reliable models to predict the effect of the manufacturing process and the induced defects on the static and fatigue performances of composite components.

Within this frame, in the present work two sets of laminates have been produced using different process parameters to obtain specimens with and without voids. Given the importance of the intra-laminar and inter-laminar properties on damage evolution of laminates, tests have been carried out to characterise the transverse cracking resistance and the mode I fracture toughness, to give a deeper insight of the relation between voids and these fundamental mechanical properties. Particular attention has been paid to the observation of damage mechanisms during the tests, with the aim to understand the role of manufacturing induced voids on the crack initiation and propagation processes.

This work represents the first step of a more extensive analysis, aimed to understand the relationships between

process parameters, defect content and morphology, and mechanical properties (mainly under fatigue loading) and integrate them for the definition of an optimal trade-off between manufacturing costs and long term performances.

Materials

The adopted reinforcement was a commercial $\pm 45^\circ$ non-crimp fabric (NCF) X-C-218 g m^{-2} -1400 mm from Saertex, made of TENAX-J STS40 F13 24K carbon fibers. A low viscosity epoxy resin, EC157 from Elantas, suitable for infusion, was used as matrix. The amminic hardener W152LR allowed a sufficiently long pot life at room temperature (two hours). The resin-to-hardener ratio, suggested by the manufacturer, was 100:30.

Two sets of laminates were produced: in the first one the resin was degassed after mixing prior to infusion and it was allowed to bleed for a long time; in the second one the resin was not degassed and the bleeding time was much shorter. These conditions led to savings in time and resin waste, but also to the presence of defects, as reported later on.

As already mentioned, both the intra-laminar and inter-laminar properties control damage initiation and evolution in multidirectional laminates, and it is important to characterise and understand how they are affected by the presence of voids.

With this aim, laminates with lay-up $[0/90]_5$ were first produced to characterise the effect of voids on the resistance to the initiation of transverse cracks.

Then, two different lay-ups, namely $[(90/0)_3]_5$ and $[(+45/-45)_3]_5$, were adopted for testing the interlaminar fracture toughness by means of DCB samples. Those two stacking sequences were considered to analyse the possible influence of the orientation of the interface plies (0 and -45°). In the DCB specimens an aluminium film (thickness $10 \mu\text{m}$) was placed between layers 6 and 7 to create a pre-crack.

Resin and hardener were mixed for 15 minutes at 300 rev min^{-1} with a DISPERMAT TU shear blender from VMA-Getzman. For producing the first set of laminates the mixing was followed by extensive degassing of the resin (at 0.05 mbar for 30 minutes), to consistently reduce the amount of air entrapped in the resin during the mixing. For the second set, the resin was not degassed. The inlet and outlet pressures were respectively 1 bar and 0.05 mbar for both sets and the infusion was carried out at room temperature. The bleeding time was measured from the time the resin reached the trap. For the first set, 10 and 15 minutes were allowed for the cross-ply and DCB laminates respectively before stopping the infusion. The different time was due to the different thickness of the two laminates. For the second set, a 3 minutes bleeding was maintained to ensure a complete filling of the fibers at a macroscopic level.

De-molding was performed after 3 days at room temperature. No post-curing was carried out on the laminates.

Static tensile tests on cross-ply laminates

Specimens were cut from the infused $[0/90]_5$ panels and tabs were bonded according to the geometry shown in Fig. 1. The

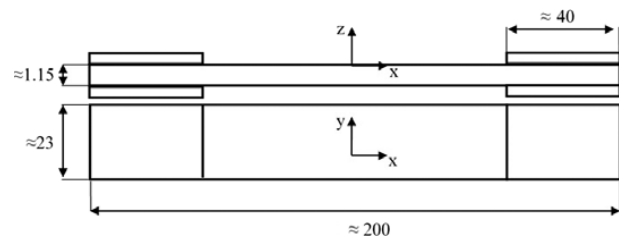


Figure 1 Geometry of cross-ply specimens (units in millimetres)

specimens were polished on both edges. No voids were found in the degassed specimens, while voids with a very irregular shape between the fibres tows were observed on the edges of the non-degassed ones, in the 90° layers, as shown in Fig. 2. The void content, in terms of void area fraction (A_v) measured on the edges, calculated by means of image analysis (carried out on 16 micrographic images), ranged between a minimum value of 1.70 and a maximum value of 4.50%, without any trend with respect to the position of the specimens in the infused panel. The voids were always found in correspondence of the polyester tows used to keep the NCF layers together. This gives reason of the irregular void shapes.

Static tensile tests were carried out on the cross-ply specimens by means of a MTS 858 MiniBionix hydraulic machine. An axial extensometer MTS632.29F-30 with an initial length of 25 mm was mounted in the central part of the specimens. Load ramps were applied in displacement control in the X-direction until progressively higher values of strain were reached (with strain steps of 0.025%). After each predefined strain level, the specimens were removed from the machine and analysed with an optical microscope, to detect the presence of edge cracks in a zone of 80 mm length centred in the specimen mid-section.

The first event of damage was always represented by the initiation of transverse cracks in the 90° layers. More and more cracks initiated as the strain level was increased. The second damage mode, occurring at higher strain levels, was the onset of macroscopic delaminations which covered tens of millimetres along the specimens length.

Each specimen was observed at both edges. In the non-degassed ones cracks were seen to initiate always in correspondence of the voids. X-Rays analyses revealed that cracks and delaminations did not propagate through the laminates width and stopped after few millimetres from the edges. This is due to the small thickness of the 90° layer, which is therefore highly constrained by the longitudinal plies, thus reducing the crack opening and, as a consequence, the energy release rate (see, for instance Ref. 36). As a consequence, transverse crack initiation was not followed by

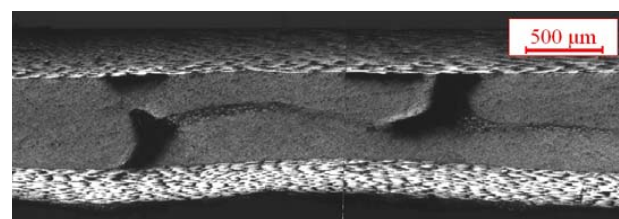


Figure 2 Example of voids in non-degassed cross-ply laminate

through the width propagation since the ERR level (even under the maximum applied strain) was too low. For this reason, the two edges of a specimen could be treated as two independent specimens. Three non-degassed and two degassed coupons were tested, and thus results are reported for six and four edges respectively.

Before analysing the damage initiation and evolution it is important to mention that no influence of the voids was found on the global elastic modulus of the laminates in the loading direction (X-direction). An average Young modulus $E_x \approx 60\,000$ MPa was found. This is a strongly fiber dominated property, and therefore not so sensitive to the presence of voids in the matrix.⁹

A first basic analysis of the influence of voids on the transverse cracking behaviour may be done by comparing the performance of void-free specimens and specimens containing voids regardless of their individual void content. The strain level after which the first crack and first macroscopic delamination were observed is reported in Fig. 3. In spite of the quite high data dispersion, the detrimental effect of the presence of voids is evident for both phenomena. In fact, the strain to first crack and first delamination initiation are decreased by respectively 20 and 14% in the presence of voids.

As already mentioned, multiple cracking occurred in all the specimens. The density of transverse cracks against the strain level is reported in Fig. 4. It is clear that for the same strain level the crack density is much higher in the presence of voids, confirming their detrimental effect on the transverse cracking behaviour.

Statistical distribution of strain to crack initiation

The influence of the presence of voids on the transverse cracking behaviour can be quantified by means of statistical considerations. If the crack density is low enough to ensure that there is no shielding effect due to the presence of multiple cracks, and if there are no delaminations, the stress and strain fields can be considered, within reason, uniform along the length of the 90° layers, their values being equal to those calculated in absence of damage. In this condition, the initiation of cracks at different strain levels is due to the presence of defects with different criticality (such as voids producing more or less severe stress concentrations) or differences in the local microstructure (such as different local fibre volume fractions, resin rich regions, waviness). From a statistical point

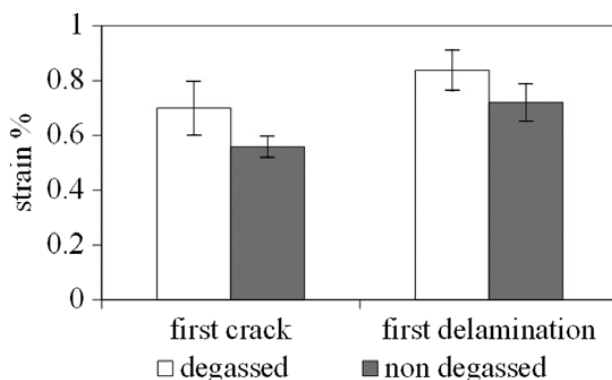


Figure 3 Strain at initiation of first crack and first delamination

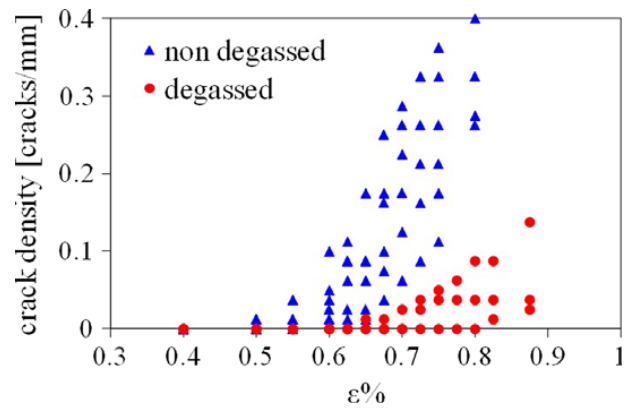


Figure 4 Crack density evolution against strain level for degassed and non-degassed cross-ply laminates

of view it can be said that along the length of the 90° layers there is a statistical distribution of the strain to crack initiation, whose cumulative probability function $P(\epsilon)$ is given by

$$P(\epsilon) = 1 - \exp \left[- \left(\frac{\epsilon}{\epsilon_0} \right)^m \right] \quad (1)$$

in which m and ϵ_0 are respectively the shape and scale parameters of the Weibull distribution.

For the determination of the parameters of the statistical distribution the procedure proposed in Ref. 19 is adopted here.

Let us divide the length of the 90° layers in small elements of length l_0 , as shown in Fig. 5. At a given value of applied strain the number of initiated cracks is equal to the number of small elements of which the strain to crack initiation is lower than or equal to the applied strain. Therefore the crack density $\rho(\epsilon)$ can be calculated as in equation (2)

$$\rho(\epsilon) = \frac{1}{l_0} \left\{ 1 - \exp \left[- \left(\frac{\epsilon}{\epsilon_0} \right)^m \right] \right\} \quad (2)$$

With the aim to provide values of the distribution parameters for a unitary length element, let us consider $l_0 = 1$ mm.

By fitting the crack density data by means of equation (2) it was possible to estimate the parameters ϵ_0 and m for the degassed and non-degassed specimens (only cracks initiated before the onset of delamination were considered in the analysis). Once the parameters are calibrated for $l_0 = 1$ mm and a given ply thickness, if a different value of l_0 or a different ply thickness are used, the cumulative probability function must be corrected to account for the volume effect. Experimental data for each edge and the fitting curves according to equation (2) are shown in Fig. 6. Crack density data for the edges of the degassed specimens are fitted all together with a single curve, as they are representative of the void-free condition. For these specimens only two of four edges are reported in Fig. 6 since in the other ones delamination occurred contemporary to the initiation of the first

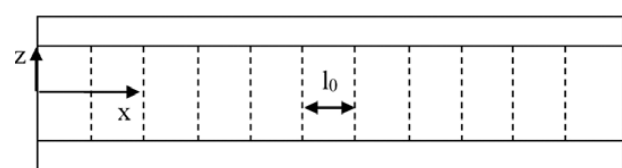


Figure 5 Subdivision of 90° layers in elements of length l_0

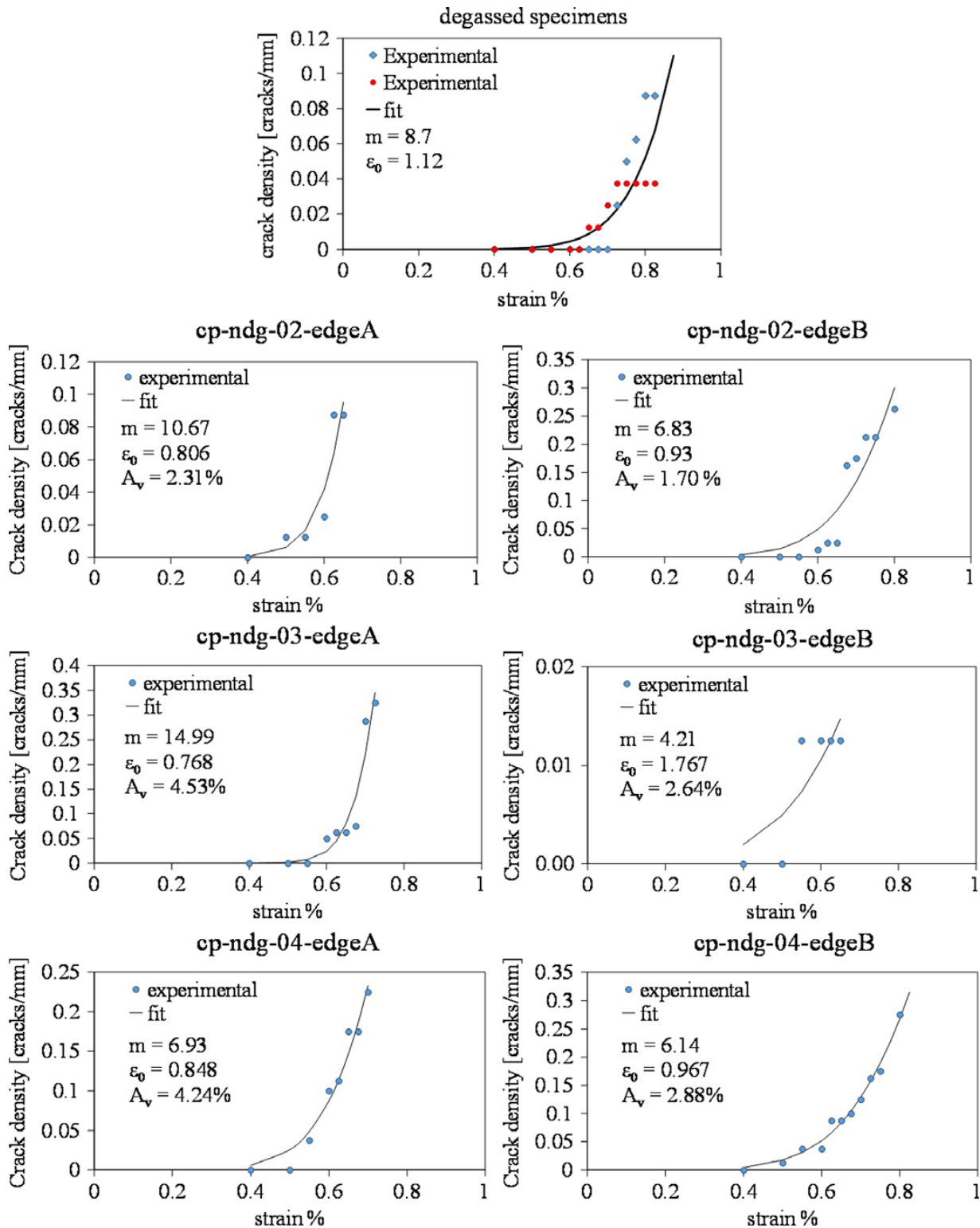


Figure 6 Crack density evolution before delamination onset and fitting curves for every edge

transverse cracks and therefore those data are not relevant for the present analysis.

The probability density functions $f(\epsilon)$, expressed in equation (3), are plotted in Fig. 7 for all the edges, using the values of m and ϵ_0 obtained by fitting the crack density curves

$$f(\epsilon) = \frac{m}{\epsilon_0^m} \epsilon^{m-1} \exp \left[-\left(\frac{\epsilon}{\epsilon_0} \right)^m \right] \quad (3)$$

The edge B of specimen cp-ndg-03, whose curve is dashed in Fig. 7, shows a behaviour not in line with the other specimens.

For this edge, however, very limited failure strain data were available, as can be seen in Fig. 6. This is due to the fact that in that edge delaminations occurred very early thus affecting the initiation of further transverse cracks. This makes this data set not relevant for the analysis of transverse cracking, and therefore it will not be considered in further analyses in the paper.

As a first attempt to correlate the presence of voids to the statistical distribution of the critical strain to crack initiation, ϵ_0 and m were related to the void content (A_v) and the linear

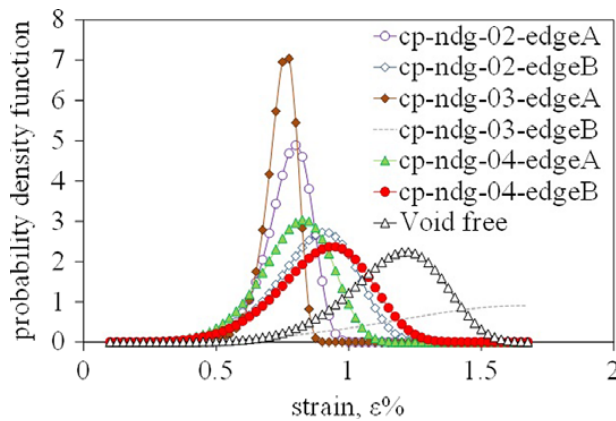


Figure 7 Probability density function for strain to crack initiation

void density of the individual edges. These two parameters are referred to as ‘global’, since they do not take into account the influence of single voids but just the global effect due to the presence of a certain amount of voids. The linear void density was defined as the ratio between the observed number of voids and the observation length (80 mm for each edge). In Fig. 8 the scale and shape parameters are plotted against these two global parameters. Clearly, no trend is appreciable concerning the influence of the void content on the shape parameter m . Conversely, the scale parameter ϵ_0 is, in general, lower for higher void contents, but it is hard to say that there is a clear and monotonically decreasing trend.

Analysis of crack initiation from voids

To better understand the influence of voids on the strain to crack initiation and to clarify some discrepancies arisen after the global statistical analysis presented in the previous section, a deeper investigation was carried out at the local level, taking into account some geometric features of the individual voids. In particular, three ‘local’ parameters were considered: the area of the voids from which a crack initiated during the

test, the corresponding section reduction of the 90° layer, and the strain concentration due to the actual shape of the voids. These local parameters were then related to the macroscopic strain at which each crack initiated from single voids.

The void area and the section reduction are plotted against the strain to crack initiation in Fig. 9a and b respectively. No trend at all can be observed in both cases, highlighting that such parameters are not adequate to describe the influence of voids on crack initiation, for the cases analysed.

A Matlab code was then developed to extract, via image analysis, the geometry of each void and the surrounding plies from a micrographic image. The code automatically produces an ANSYS APDL file with the geometry to be used for a 2D stress analysis with the finite element code ANSYS 14.0. In the FE analyses the plies were treated as homogeneous and orthotropic, a generalized plain strain condition was assumed and displacement boundary conditions were applied as schematically shown in Fig. 10. Eight nodes plane element were used (PLANE 183 in the Ansys library) whose dimension was chosen, after a dedicated convergence analysis, to be about 1/35 of the 90° ply thickness.

As voids are located in the inter-tow regions, it is reasonable to assume that their shape is quite elongated in the fibres direction of the 90° ply. For this reason, a 2D analysis could be appropriate, even if not exactly representative of the real geometry, mainly considering that this analysis is aimed to understand qualitatively which is the most critical feature of a void that leads to the initiation of a transverse crack.

An example of analysis is reported in Fig. 11, where a micrograph and a void reconstruction are shown. The first principal strain field is also shown in the 90° ply, showing an excellent agreement between the crack initiation site and the peak point of the maximum principal strain.

The calculated strain concentration factors (ratio between the peak strain at the void and the global strain) for all the voids that lead to transverse cracks before the onset of delaminations are plotted in Fig. 12 against the global strain

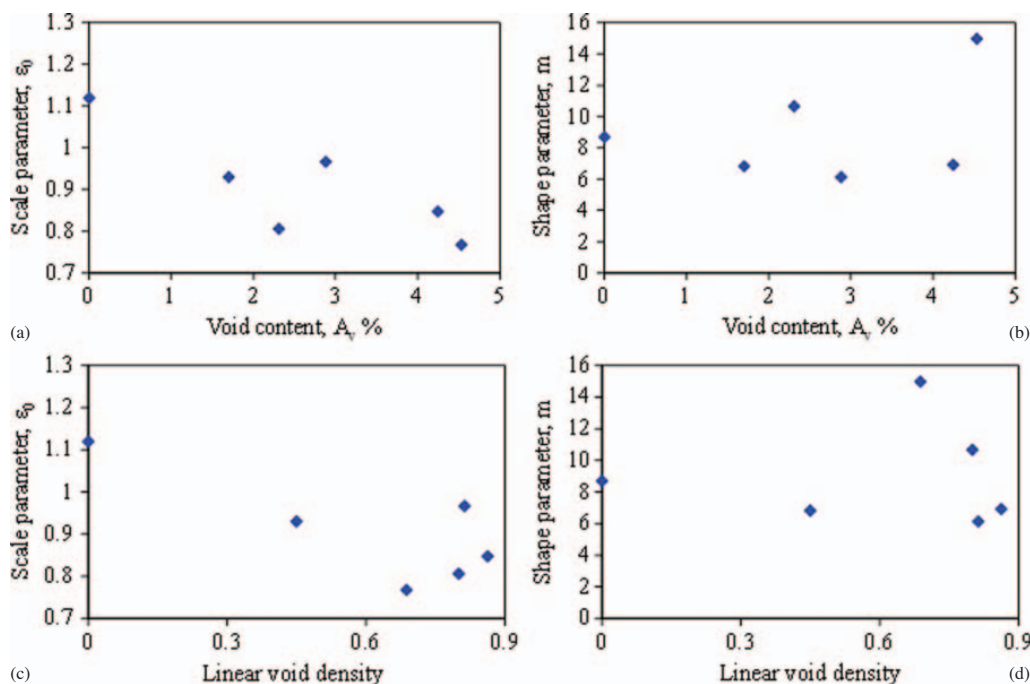


Figure 8 Weibull scale and shape parameters as function of void content and linear void density (‘global’ parameters)

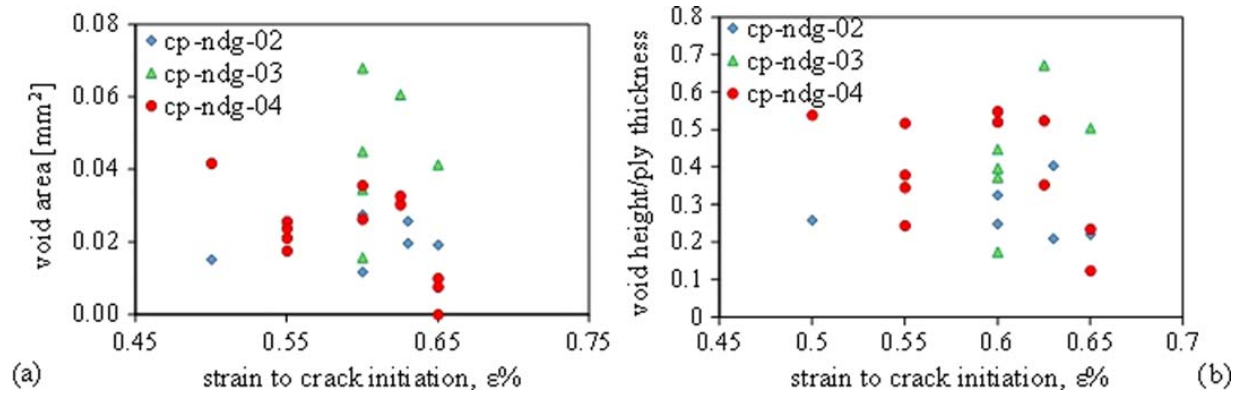


Figure 9 a void area and b section reduction due to presence of void plotted against strain to crack initiation

to crack initiation. In spite of the considerable data scatter a clear decreasing trend can be observed. An analysis of variance (one-way ANOVA) confirmed that there is a statistically significant influence of the void shape (and the strain concentration it causes) on the global strain level at which cracking occurs, as shown in Table 1. The *null hypothesis*, that consists of assuming no influence of the strain concentration, is rejected as the F value is larger than the critical F value, calculated for a significance level $\alpha = 0.01$ (see Ref. 37 for detailed explanations of the required calculations). This result means that in the presence of such irregularly shaped inter-tow defects the very local geometry of the voids and the surrounding plies, and the relevant strain concentration, are fundamental to be accounted for to predict the global strain or stress for crack initiation. This explains the results shown in Fig. 8a and c, where a global decreasing trend was highlighted for the scale parameter against the void content (even if some discrepancies were found). In fact, if the void content is higher there is a higher probability to find higher stress or strain concentrations, and this explains the globally decreasing trend. However, a global parameter such as the void content is not enough to describe the phenomenon in a detailed and completely reliable way, since the local shape of the voids has been found to play a fundamental role in the crack initiation phenomenon. Even if this conclusion has been drawn for the initiation of transverse cracks at the edges, the authors believe that it can be qualitatively extended for cracks initiating in other regions of a laminate.

DCB tests

As mentioned in the introduction and shown in the previous section, transverse cracking is followed by the onset and propagation of delamination. This phenomenon is controlled

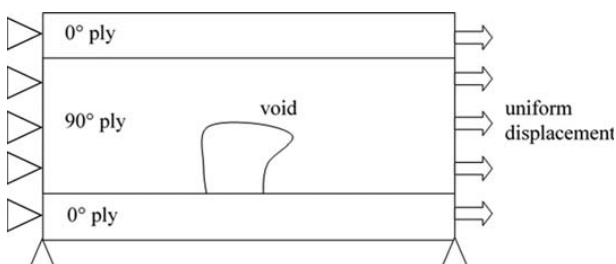


Figure 10 Schematic of displacement boundary conditions for FE analysis

by the interlaminar fracture toughness, and the presence of voids can have a significant influence on this property.

To understand the effect of the manufacturing process on the mode I interlaminar fracture toughness, static DCB tests were carried out on degassed and non-degassed specimens with two different stacking sequences ($[(90/0)_3]_s$ and $[(\pm 45)_3]_s$). This allowed us to analyze also the influence of the orientation of the interface layers (0° or -45°). Test specimens were cut from the infused panels according to the geometry shown in Fig. 13.

Tests were carried out with a MTS 858 MiniBionix hydraulic machine in displacement control with a crosshead rate of 2 mm min^{-1} . The crack length a was measured during the test with the aid of a travelling optical microscope ($\times 40$). The applied loads and displacements were recorded during the tests and the mode I energy release rate (ERR) G_I , was calculated by means of the Compliance Calibration method as proposed in the ASTM recommendations.³⁸

0° interface

The edges of the $[(90/0)_3]_s$ DCB specimens were polished and observed under an optical microscope, revealing the presence of voids only in the non-degassed ones, as can be seen in Fig. 14 (average void area fraction: 1.9%). In addition to the inter-tow voids some very elongated voids can be observed in the 0° tows, as indicated by the zoom in Fig. 14.

The R-curves for the 0° interface specimens are shown in Fig. 15. The specimens obtained with degassed and non-degassed resin are indicated, respectively, with the codes DCB-DG and DCB-NDG. The initiation values (for $a - a_0 = 0$) correspond to the values at which the crack is seen to start propagating from the pre-crack front. The curves exhibit the typical increasing trend in the first part and then a plateau for $a - a_0 > 10 - 15 \text{ mm}$. It can be seen that, after the first part in which the curves for degassed and non-degassed specimens are overlapped, the specimens with voids exhibit a slightly higher value of the critical ERR for crack propagation. This beneficial effect of voids is in agreement with the results obtained by Asp and Brandt⁵ and is actually due to the fact that the presence of voids gives rise to a more complicated crack path and a more diffused damage, so that a higher energy has to be supplied to make the crack propagate. In particular, in this case, the presence of voids led to a more diffused fibre bridging. In fact, as shown in Fig. 16, secondary

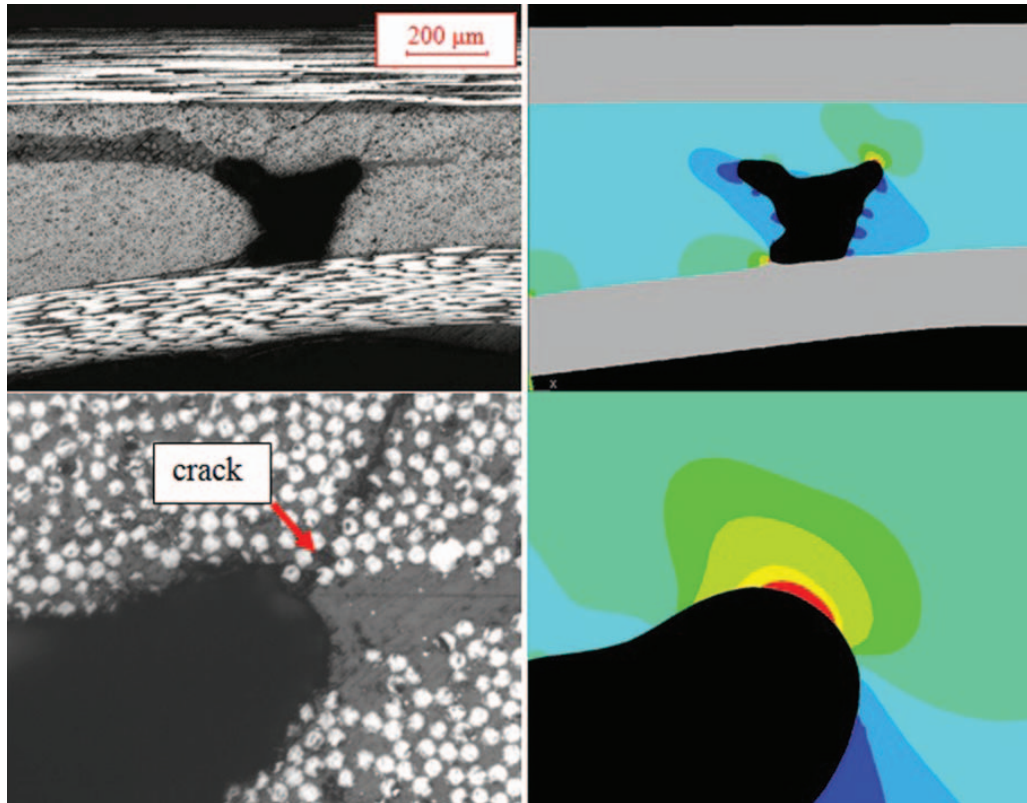


Figure 11 Example of principal strain plot in FE analysis carried out on geometry extracted from micrographic image

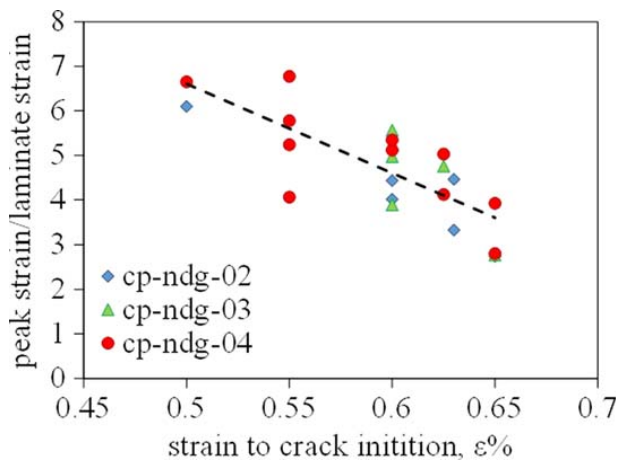


Figure 12 Peak strain, normalised to laminate strain, plotted against strain to crack initiation

cracks initiated close to the elongated voids in the 0° plies then promoting the fiber bridging phenomenon as the main crack propagated and joined the void.

45° interface

Microscopy observations were carried out at the edges of the [(±45)₃]_s specimens, revealing, again, the complete absence

of voids in the degassed ones. Conversely, an average void area fraction of 1.23% was observed on the edges of the non-degassed specimens. Voids were uniformly distributed along the specimen length and positioned between the tows of the carbon fibre NCF, as shown in Fig. 17.

The R-curves presenting the critical value of the mode I ERR G_{Ic} against the crack increment, are shown in Fig. 18. In this case a slightly higher values of the critical ERR has been obtained for non degassed specimen both for crack initiation and propagation. In particular, voids produced deviations of the main crack path as well as secondary cracks initiating from the voids themselves, thus causing a more diffused ply-bridging phenomenon, as shown in Fig. 19.

DCB fatigue tests

For the 0° interface specimens, fatigue tests were also carried out to understand the influence of voids on the crack growth rate (CGR) under mode I loading.

Two void-free specimens and two specimens with 1.9% void area fraction were tested under displacement control with a frequency of 8Hz and a load ratio (minimum to maximum load ratio) of 0.1. Crack growth data were analysed according to the IPM procedure suggested in the recommendation ASTM E647-00³⁹ and presented in Fig. 20. The CGR is here plotted against the maximum cyclic value of

Table 1 One-way ANOVA to assess influence of void geometry on crack initiation strain

Source of variation	Sum of squares (SS)	Degrees of freedom	Mean square (MS)	F	Significance	Critical F ($\alpha = 0.01$)
Between groups	20.09	5	4.018	7.73	0.000595	4.34
Among groups	8.84	17	0.520			
Total	28.93	22				

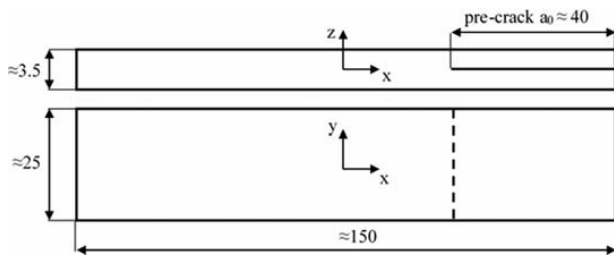


Figure 13 Geometry of DCB specimens (units in millimetres)

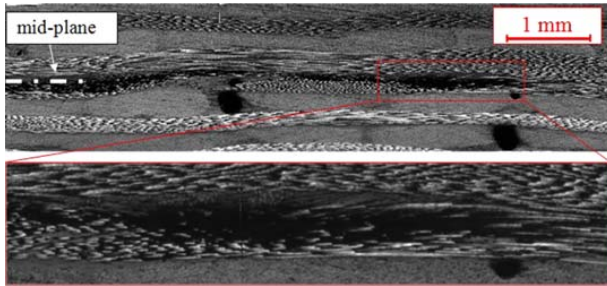


Figure 14 Voids in non-degassed [(90/0)₃]_s DCB specimen before tests

G_I . Typical S-shaped curves are obtained, and no appreciable difference can be noticed between the degassed and non degassed specimens. The threshold condition is reached for $G_{I,max}$ equal to about 0.08 kJ m^{-2} , while a rapid increase in the CGR occurs for maximum ERR values around 0.3 kJ m^{-2} , in good agreement with the static initiation value.

Concerning fatigue loading, the comparable behaviour of specimens with and without voids is consistent with the fact that secondary cracks and fibre bridging were not observed during the tests, as instead happened under static loading.

Conclusions

Infused laminates were produced by a carbon fiber NCF and epoxy matrix adopting two different processes: in the first one the matrix was completely degassed before infusion and



Figure 17 Voids in non-degassed [(±45)₃]_s DCB specimen before test

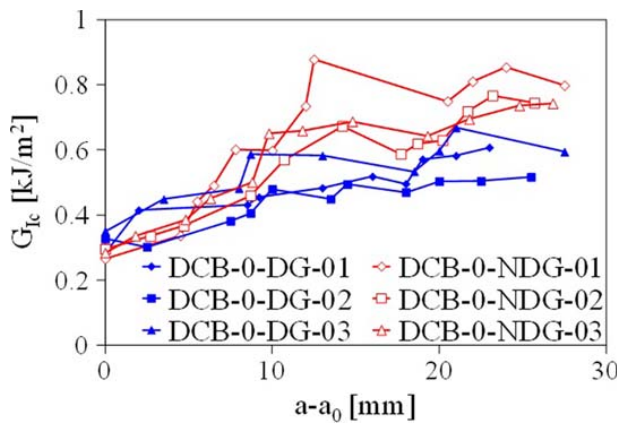


Figure 15 R-curves for 0° interface DCB specimens

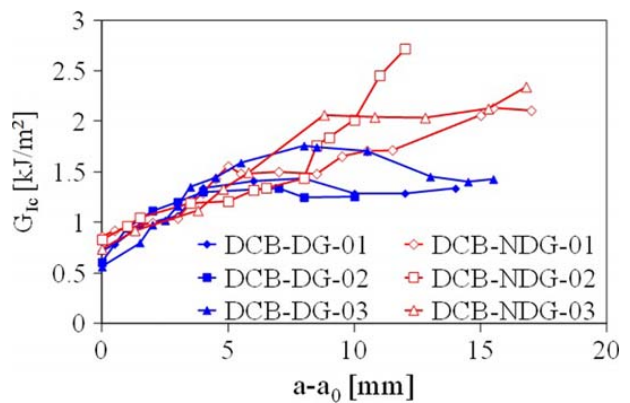


Figure 18 R-curves for degassed and non-degassed [(±45)₃]_s DCB specimens

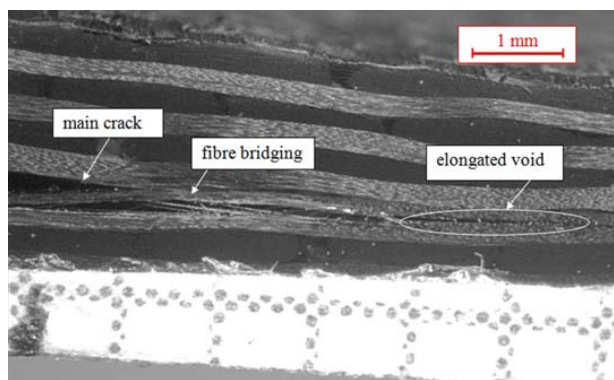


Figure 16 Secondary cracks and consequent fiber bridging due to presence of elongated voids

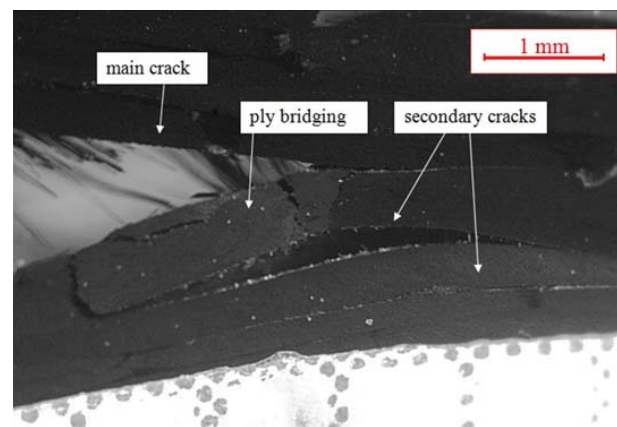


Figure 19 Secondary cracks and ply bridging due to the presence of voids

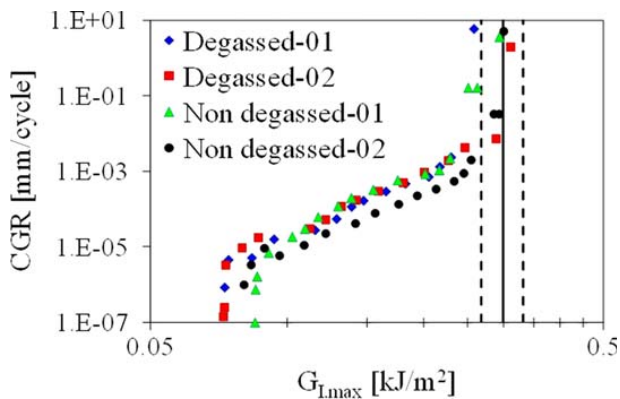


Figure 20 Paris-like curves for degassed and non-degassed DCB specimens

a long bleeding time was adopted to optimise the pre-form filling; in the second one the matrix was not degassed and a minimum bleeding time was adopted. The last process led to savings in time and resin waste, but caused the diffuse presence of voids, mainly between the tows of the NCF. Experimental tests were carried out to characterise the influence of voids on some intra- and inter-laminar properties, focusing on the observation of damage mechanisms and their dependence on the presence of voids.

The following main conclusions can be drawn.

1. The strain to the initiation of the first transverse crack at the edges and the first delamination, as well as the edge crack density evolution in cross-ply laminates, were found to be detrimentally affected by the presence of voids.
2. The statistical distribution of the strain to crack initiation depends on the global void content, but a clear monotonic trend was not observed.
3. The very local shape of the voids, and the related strain concentration, are fundamental parameters to describe the influence of such voids on the strain to crack initiation.
4. In the cases analysed, the critical value of G_{IC} for inter-laminar crack propagation was slightly higher in the specimens containing voids. In fact, while voids lying on the interface at which crack is propagating are expected to facilitate its propagation, voids away from it are source of more complicated crack paths and more pronounced fibre or ply bridging increasing the apparent fracture toughness.

Conflicts of interest

The authors have no conflicts of interest to declare.

References

1. V. Rohatgi, N. Patel and L. James Lee: *Polym. Compos.*, 1996, **17**, (2), 161–170.
2. M. K. Kang, W. I. Lee and K. T. Hahn: *Compos. Sci. Technol.*, 2000, **60**, 2427–2434.
3. N. Kuentzer, P. Simacek, S. G. Advani and S. Walsh: *Compos. A-Appl. S.*, 2007, **38**, 802–813.
4. V. R. Kedari, B. I. Farah and K. T. Hsiao: *J. Compos. Mater.*, 2011, **45**, 2727–2742.
5. L. E. Asp and F. Brandt: 'Effects of pores and voids on the interlaminar delamination toughness of a carbon/epoxy composite', Proc. ICCM11, Gold Coast, Queensland, Australia, July 1997, 322–331.
6. P. A. Olivier, B. Mascaró, P. Margueres and F. Collombet: 'CFRP with voids: ultrasonic characterization of localized porosity, acceptance criteria and mechanical characteristics', Proc. ICCM16, Kyoto, Japan, July 2007.
7. H. Yoshida, T. Ogasa and R. Hayashi: *Compos. Sci. Technol.*, 1986, **25**, 3–18.
8. J. M. Tang, W. I. Lee and G. S. Springer: *J. Compos. Mater.*, 1987, **21**, 421–440.
9. P. Olivier, J. P. Cottu and B. Ferret: *Composites*, 1995, **26**, 509–515.
10. J. L. Thomason: *Composites*, 1995, **26**, 467–475.
11. M. R. Wisnom, T. Reynolds and N. Gwilliam: *Compos. Sci. Technol.*, 1996, **56**, 93–101.
12. A. A. Goodwin, C. A. Howe and R. J. Paton: 'The role of voids in reducing the interlaminar shear strength in RTM laminates', Proc. ICCM11, Gold Coast, Australia, July 1997, 11–19.
13. M. L. Costa, S. F. M. de Almeida and M. C. Rezende: *Compos. Sci. Technol.*, 2001, **61**, 2101–2108.
14. M. N. Bureau and J. Denault: *Compos. Sci. Technol.*, 2004, **64**, 1785–1794.
15. L. Liu, B. M. Zhang, D. F. Wang and Z. J. Wu: *Compos. Struct.*, 2006, **73**, 303–309.
16. H. Zhu, D. Li, D. Zhang, B. Wu and Y. Chen: *T. Nonferr. Metal Soc.*, 2009, **19**, 470–475.
17. J. Varna, R. Joffe, L. A. Berglund and T. S. Lundstrom: *Compos. Sci. Technol.*, 1995, **53**, 241–249.
18. H. Zhu, B. Wu, D. Li, D. Zhang and Y. Chen: *J. Mater. Sci. Technol.*, 2011, **27**, (1), 69–73.
19. Y. Huang, J. Varna and R. Talreja: *Compos. Sci. Technol.*, 2014, **95**, 100–106.
20. J. C. Suarez, F. Molleda and A. Guemes: 'Void content in carbon fiber/epoxy resin composites and its effects on compressive properties', Proc. ICCM9, Madrid, Spain, July 1993, 589–596.
21. J. Cinquin, V. Triquenaux and Y. Rouesne: 'Porosity influence on organic composite material mechanical properties', Proc. ICCM16, Kyoto, Japan, July 2007.
22. A. R. Chambers, J. S. Earl, C. A. Squires and M. A. Suhot: *Int. J. Fatigue*, 2006, **28**, 1389–1398.
23. S. F. M. de Almeida and Z. S. N. Neto: *Compos. Struct.*, 1994, **28**, 139–148.
24. P. O. Hagstrand, F. Bonjour and J. A. E. Manson: *Compos. A-Appl. S.*, 2005, **36**, 705–714.
25. C. W. Dill, S. M. Tipton, E. H. Glaessgen and K. D. Branscum: 'Fatigue strength reduction imposed by porosity in a fiberglass composite', in 'Damage detection in composite materials', (ed. J. E. Masters), Issue 1128 152–162; 1992, Philadelphia, PA, ASTM International.
26. F. Schmidt, M. Rheinfurth, P. Horst and G. Busse: *Int. J. Fatigue*, 2012, **43**, 207–216.
27. F. Gehrig, E. Mannov and K. Schulte: 'Degradation of NCF-epoxy composites containing voids', Proc. ICCM 17, July 2009.
28. M. A. Suhot and A. R. Chambers: 'The effect of voids on the flexural fatigue performance of unidirectional carbon fibre composites', Proc. ICCM16, Kyoto, Japan, July 2007.
29. J. Lambert, A. R. Chambers, I. Sinclair and S. M. Spearing: *Compos. Sci. Technol.*, 2012, **72**, 337–343.
30. G. Seon, A. Makeev, Y. Nikishkov and E. Lee: *Compos. Sci. Technol.*, 2013, **89**, 194–201.
31. S. Sisodia, E. K. Gamstedt, F. Edgren and J. Varna: *J. Compos. Mater.*, DOI 10.1177/0021998314541993.
32. A. J. McMillan: *J. Reinf. Plast. Comp.*, 2012, **31**, (1), 13–28.
33. H. Huang and R. Talreja: *Compos. Sci. Technol.*, 2005, **65**, 1964–1981.
34. B. Van Den Broucke, J. Hegemann, R. Das, R. Oster, K. Hackl and R. Stöbel: 'Modelling of textile composites using finite element tools and investigation of the influence of porosity on mechanical properties', Proc. Symp. 'Finite element modelling of textiles and textile composites', St Petersburg, Russia, September 2007, 1–7.
35. M. Ricotta, M. Quaresimin and R. Talreja: *Compos. Sci. Technol.*, 2008, **68**, 2616–2623.
36. M. Quaresimin, P. A. Carraro, L. P. Mikkelsen, N. Lucato, L. Vivian, P. Brøndsted, B. F. Sørensen, J. Varna and R. Talreja: *Compos. B-Eng.*, 2014, **61**, 282–290.
37. D. C. Montgomery: 'Design and analysis of experiments', 8th edn; 2012, New York, John Wiley & Sons.
38. 'Standard test method for mode I interlaminar fracture toughness of unidirectional fiber-reinforced polymer matrix composites', ASTM D 5528-01, Philadelphia, PA, USA, 2007.
39. 'Standard Test method for measurement of fatigue crack growth rates', ASTM E647-00, Philadelphia, PA, USA, 2000.